

Cost-Optimal Operation for a Flexible Building with Local PV in a Singaporean Environment

Sarmad Hanif^{1,2*}, Christoph Gruentgens^{1†}, Tobias Massier^{1‡}, Thomas Hamacher^{3§}, Thomas Reindl^{2¶}

¹TUM CREATE Limited, Singapore 138602

²Solar Energy Research Institute of Singapore (SERIS), National University of Singapore (NUS), Singapore 117574

³Technical University of Munich (TUM), Garching 85748, Germany

*sarmad.hanif@tum-create.edu.sg, †christoph.gruentgens@rwth-aachen.de, ‡tobias.massier@tum-create.edu.sg,

§thomas.hamacher@tum.de, ¶thomas.reindl@nus.edu.sg

Abstract—In the future, flexible demand with the combination of renewable energy may hold the key for a sustainable power grid. However, if not managed properly, this combination may pose a threat to the reliability of the grid. In this paper, we analyze the effect on the cost-optimal operation of the flexible building in the presence of locally connected solar photovoltaic (PV) system. Based on a detailed thermal model of a building, an optimization based operational strategy has been presented. The objective of this strategy is to optimally schedule energy and reserve in the presence of flexible loads and the PV system. Two forecasting methods, in a rolling horizon fashion, are deployed to evaluate the interaction between the uncertain PV output and the operation of the whole system. Case studies are performed using the pricing framework of the National Energy Market Singapore (NEMS). Results show that a trade-off exist between the cost optimality of the overall system and the excess PV output fed to the grid (reverse power flow).

Index Terms—Demand Response, Buildings, Reverse Power Flow, Forecasting Methods, Photovoltaic, Cost Optimal.

I. INTRODUCTION

Taking into account the increased awareness for reducing greenhouse gas emissions, renewable energy offers a cleaner alternative to fossil fuels. For Singapore, distributed PV apparently is the only feasible renewable option [1]. Aside from its positive effects, due to its limited controllability, the installation of distributed PV entails new challenges. An extremely important one being the power flowing back into the grid i.e. reverse power flow [2]. This happens during times of high solar irradiation, when power generated by PV installations is higher than the local consumption of connected loads. In principle, reverse power flow induces 3 major issues in the distribution grid: (1) over voltage at the point of connection, (2) transformer overloading, and (3) higher overall losses.

Another interesting option for improving the overall efficiency of energy systems is the introduction of demand response (DR) programs [3], [4]. Aside from other objectives, DR also helps to mitigate the variability of renewables. In Singapore, the Energy Market Authority (EMA) has issued instructions for the deployment of the DR program [5]. Buildings, due to high consumption share and inherent thermal inertia, present as a natural candidate for providing flexible demand. Although building owners would like to avail the DR program to achieve a cost effective operational strategy, however, this flexible demand can also coordinate with the

locally connected PV system. In this way, the variability of PV system may be limited, improving building's operational cost as well as the reverse power flow at the point of common coupling's (POCC).

With respect to this paper, the closest work in the existing literature has been reported in [6]–[10]. In [10], authors considered the PV hosting capacity for the whole grid, whereas in [6], deployment of storage devices was considered. Nevertheless, the analysis was conducted on the residential sector, not translatable to commercial buildings. The published work in [7], [9] focused on buildings, but comments regarding the effect on the self consumption of PV strategy under imperfect conditions were not found. In [8], authors discussed the regulation and energy efficiency aspects of buildings. Hence, according to the knowledge of authors, there has not been any published work, which points out the connection between the cost optimality of the energy procurement strategy by the flexible building and its effect on the reverse power flow.

Hence, the contribution of this paper is threefold. First, we present a cost-optimal moving horizon control strategy considering options to: (1) shift energy or provide interruptible load (reserves) and (2) consume or sell back the rooftop PV to the grid. Second, the effect on the developed control strategy due to the inclusion of imperfect forecasts is also discussed. Third, a quantitative analysis is performed regarding the operating cost of energy procurement and its relationship with the self consumption of PV.

Section II explains the modeling procedure. The cost-optimal model predictive control (MPC) strategy with the real-time adjustment to account for imperfect PV forecast is explained in Section III. Section IV and Section V provides the simulation results and discussion of this paper.

II. MODELING ENVIRONMENT

A. Market Setting

In NEMS, for a flexible contestable building with a locally connected solar PV, the following options exist:

1) *Demand Shifting & Interrupting*: The loads are allowed to bid for reserves and energy provision through the Interruptible Load (IL) [11] and the DR [5] programs, respectively. The payment for DR program is based on the overall load/price reduction of the grid, whereas the IL are remunerated with

respect to the reserve price of the market. Since we focus only on one building in this paper, it is assumed that payments for the modeled system is based on the uniform Singapore energy price (c_k) and reserve price (z_k), provided by the Energy Market Company (EMC) [5], [12], [13].

2) *PV Settlement*: In Singapore, for a contestable consumer with less than 1MWac embedded PV, two options exist for registering its system: (1) with Singapore Power Grid (SP) [14], or (2) with the EMC [12]. For this paper, it is assumed that the flexible building is operated under option 2. This means that the excess PV fed back to the grid is compensated based on the nodal price n_k of the respected region.

B. Building Model

In our previous work [15], a single zone (room) model, adopted from [16], was augmented to generate the model for a whole building. Since the investigation for the aggregation of buildings was performed, the proposed approach achieved an adequate balance between the complexity and simplicity of the model. Since here we only focus on a single building; a more involved procedure, using a building-resistance capacitance modeling (BRCM) toolbox, is adopted [17].

The advantage of the BRCM toolbox lies in its ability to separate the dynamic thermal model (heat transfer between rooms, walls etc.) and the static external heat flux (EHF) model (solar and internal gains etc.) of the building. The BRCM models the interaction of thermal states (temperatures), $x_t^b \in \mathbb{R}^{n_x}$ with the aggregated EHF inputs, q_t^b as:

$$\dot{x}_t^b = A_t^b x_t^b + B_t^b q_t^b(x_t, u_t, v_t). \quad (1)$$

Where t , represents the thermal model. In principle, q^b can be considered as a response in the form of heat, due to the influence of control inputs ($u_t^b \in \mathbb{R}^{n_u}$) and disturbances ($v_t^b \in \mathbb{R}^{n_v}$) on the system. Indices n_x , n_u and n_v represent the number of states, inputs and disturbances considered in the model. The thermal model in (1) is discretized,

$$x_{k+1}^b = A^b x_k^b + B_u^b u_k^b + B_v^b v_k^b + \sum_{i=1}^{n_u} (B_{v_u,i}^b v_k^b + B_{x_u,i}^b x_k^b) u_{k,i}^b, \quad (2)$$

to obtain a bilinear model of the system (the time varying product of states and disturbances with control inputs)¹. In order to linearize it, 2 simplifications are proposed: (1) it is assumed that the temperature experienced by the outside of the walls, solar irradiation and heat gains are known in advance, (2) only the HVAC's mass flow is taken as a control input. Under these assumptions, the input dependent state $B_{x_u}^b$ and disturbance $B_{v_u}^b$ matrices collapse into the A^b and B^b , respectively. The model is also extended to provide IL, by introducing a reserve vector r_k^b . The resultant discrete time linear state space model is represented as:

$$x_{k+1}^b = A^b x_k^b + B_u^b (u_k^b + r_k^b) + B_v^b v_k^b \quad (3)$$

In (3), the dimensions of the vectors are: $x_k^b \in \mathbb{R}^{n_x \cdot n_f}$,

¹Please refer to [17] for the information regarding more insight into the thermal model and its corresponding matrices.

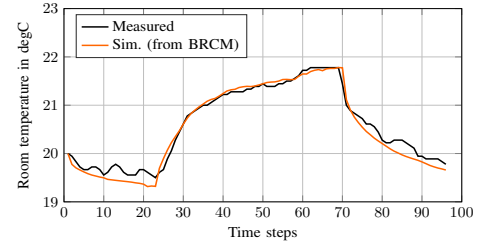


Fig. 1. Validation of the BRCM toolbox with actual measurement from [16]

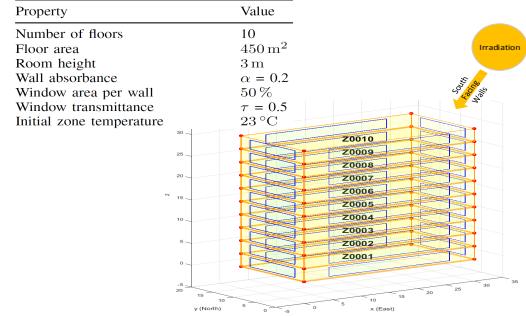


Fig. 2. Assumed property values of the modeled building

$u_k^b \in \mathbb{R}^{n_u \cdot n_f}$ and $v_k^b \in \mathbb{R}^{n_v \cdot n_f}$, with n_f as the number of floors of the building. As a validation, Fig. 1 shows the comparison between the simulated zone model (from the BRCM) and measured temperature (from [16]). It can be observed that the BRCM toolbox shows a close similarity to the actual temperature evolution. This validation enforces that the BRCM provides an extensible, yet comprehensive, tool for modeling the thermal dynamics of a building [17].

Using the procedure described above, a Singaporean office building is modeled. The values for the ambient temperature and solar irradiation are taken from the actual measurement station operated by the Solar Energy Research Institute for Singapore (SERIS) [18]. Figure 2 shows the assumed property values used to develop the building model.

C. Warm Water Storage Model

The Warm Water Storage (WWS) model is considered to provide flexibility in the consumption of the building's warm water demand. In order to align with the above described modeling philosophy for the building, the WWS is also modeled as a discrete-time linear state space system. For each step k , the temperature evolution of the water storage tank (x_k^w), due to the supplied heat ($u_k^w + r_k^w$), the ambient temperature (v_k^w), and building's warm water demand (d_k^w) is modeled as:

$$x_{k+1}^w = A^w x_k^w + B_u^w (u_k^w + r_k^w) + [B_v^w \quad B_d^w] \begin{bmatrix} v_k^w \\ d_k^w \end{bmatrix} \quad (4)$$

where,

$$A^w = (1 - \frac{kA}{mc_p})\Delta t, \quad B_u^w = \frac{\Delta t}{mc_p}, \quad B_v^w = \frac{kA\Delta t}{mc_p}.$$

Δt represents a constant discretized interval. Since the building is assumed to contain one storage tank, all variables in (4) are scalar. Table I shows the adopted values for constructing the WWS model [19].

D. PV Model

For the PV model, it is assumed that the net power supplied per unit collector surface area (u_k^i) is directly proportional to the irradiation measurements from SERIS [18]. The total power supplied u_k^{pv} by the PV model is

$$u_k^{pv} = u_k^i A_{pv} \eta_{pv}. \quad (5)$$

Please refer to Table I for the assumed values of the PV model.

Table I
PARAMETER VALUES FOR THE WWS AND PV MODEL

Mass of the tank (m)	300 kg
Surface area of the tank (A)	7 m ²
Specific heat capacity (c_p)	4.18 kJ kg ⁻¹ K ⁻¹
Heat transfer coefficient (k)	1.92 W m ⁻² K ⁻¹
Initial temperature (x_0^w)	80 °C
Warm water demand (d_k^w) (day/night)	16 kW / 2 kW
PV collector area A_{pv}	400 m ²
PV system efficiency η_{pv}	12 %

E. Overall System Model

The state space model for the whole system can be compactly represented by augmenting (3) and (4).

$$x_{k+1} = Ax_k + B_u(u_k + r_k) + B_v v_k \quad (6)$$

The overall system model (6) distinguishes between the energy consumed by the PV and the grid (7a). In (7b), u_k^{pv} and $u_k^{pv_e}$ represent the total PV production and the excess energy fed by PV back into the grid.

$$u_k = \begin{bmatrix} u_k^{b,pv} + u_k^{b,g} \\ u_k^{w,pv} + u_k^{w,g} \end{bmatrix} \quad (7a)$$

$$u_k^{pv} = u_k^{b,pv} + u_k^{w,pv} + u_k^{pv_e} \quad (7b)$$

In (7), as well as throughout the paper, superscripts “g”, “pv”, “b”, “wvs” stand for the input power from/for the grid, PV system, building and WWS, respectively.

F. Forecast Error

The solar irradiation can not be predicted accurately. The imperfect forecast effects the prediction of both the building and the PV model. Hence, in order to account for these uncertainties, two types of forecasting errors are included.

1) *Stochastic Error*: The idea of this forecast originated from [10], [20]. An increase in the error of the forecast is assumed over the length of the horizon. This means that error in the forecast increases linearly with a specific mean (μ) and overestimation/underestimation (σ^+/σ^-) variance. For the case of this paper, the maximum value of μ , and intraday σ^+ and σ^- are assumed to be 20%, 30% and 20%, respectively [20]. Random integers (+1, -1) are used to randomly choose between the over (+1) and underestimated (-1) error values.

2) *Worst Case Error*: To account for the worst case scenario, this method adjusts forecast error values of the previous method ($u_k^{pv+} = \max(u_k^{pv}, 0)$).

Please note that due to the incorporation of the rolling horizon control strategy (see Section III), some disturbances experienced by the modeled system are automatically rejected. But there are two main motivations, which necessitate the analysis of the developed MPC under different forecast errors. First, due to the participation in the DR and IL programs, self consumption from PV may effect the cost estimation of load operators, and failure to meet the scheduled load may impose heavy penalties from the operator. Second, the deviation in the optimal objective also introduces an uncertainty in the reverse power flow at the POCC.

III. OPERATIONAL STRATEGY

Figure 3 depicts the basic control strategy of this paper. For the whole time horizon N , the following procedure is repeated at each time step k :

- 1) Based on the inputs, the MPC obtains the cost-optimal energy/reserve (u_k/r_k) and PV (u_k^{pv}) schedules (see Section III).
- 2) For the case of mismatch ($\Delta u_k^{pv_m} = u_k^{pv} - u_k^{pv_m}$) between the predicted (u_k^{pv}) and actual PV output ($u_k^{pv_m}$), real time adjustment procedure is invoked²:
 - a) If shortage in the PV forecast is observed ($\Delta u_k^{pv_m} \leq 0$).
 - i) If the self PV consumption schedule is violated
 - A) Then purchase the missing energy from the grid ($u_k^{pv_{sh,s}}$).
 - B) Else adjust the shortage of the PV output, scheduled to be fed back to the grid ($u_k^{pv_{sh,a}}$).
 - b) If excess in the PV forecast is observed ($\Delta \geq u_m^{pv}$)
 - i) Then adjust the excess PV output, scheduled to be fed back to the grid ($u_k^{pv_{e,a}}$).

Cost Optimization

The cost optimization of the MPC is performed as:

$$\min_{u^*, r^*, u^{*pv_e}} \sum_{k=0}^{N-1} c_k u_k + (c_k - z_k) r_k - n_k u_k^{pv_e} + \rho \epsilon_k \quad (8a)$$

subject to

$$x_{k+1}^c = Ax_k^c + B_u u_k + B_v v_k \quad (8b)$$

$$x_{k+1}^{nc} = Ax_k^{nc} + B_u(u_k + r_k) + B_v v_k \quad (8c)$$

$$x_k^- - \epsilon_k \leq x_k \leq x_k^+ + \epsilon_k \quad (8d)$$

$$u_k^- \leq u_k + r_k \leq u_k^+ \quad (8e)$$

$$0 \leq u_k^{b,pv} + u_k^{w,pv} + u_k^{pv_e} \leq u_k^{pv} \quad (8f)$$

$$u_k - r_k, r_k, \epsilon_k \geq 0 \quad \forall k = 0, 1, \dots, N-1 \quad (8g)$$

Please note that in this context, optimality is measured in terms of the minimization of the total cost. This linear optimization

²The superscripts “e”, “sh”, “s” and “a” denotes excess, shortage, settled and adjusted PV outputs.

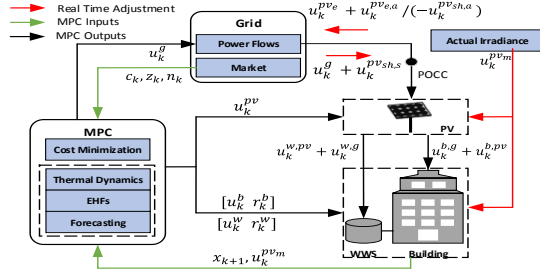


Fig. 3. The interaction of the MPC with the market, grid and building.

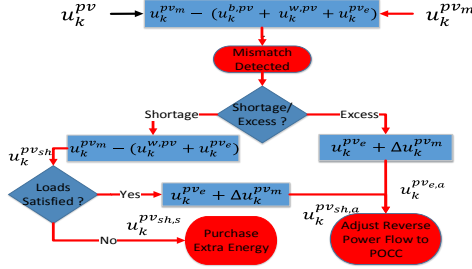


Fig. 4. Real time adjustment procedure to adjust and settle the cost-optimal schedule from the MPC.

problem results in the schedule for the optimal energy (u^*), reserve (r^*), and PV to be fed back to grid ($u_k^{pv_e}$). From the whole sequence, only the current inputs (u_0^* , r_0^* , u^{*pv_e}) are applied to the system, and the optimization is repeated again with updated states. Due to the inclusion of ILs, state trajectories for both of the curtailed (8b) and non-curtailed (8c) are kept feasible (8d). To avoid infeasibility of the solution, temperature constraints are softened by using a slack variable ϵ_k . The slack is then penalized in the objective function using an arbitrarily large constant ρ . Actuator limits of the whole model are constrained in (8e).

IV. SIMULATION RESULTS

The proposed operational strategy of Section III is evaluated for three cases. Case 1 represents the benchmark cost-optimal strategy, that means without considering any uncertainty in the PV forecast. Case 2 and 3 consider imperfect PV forecast, following the method described in Section II-F1 and Section II-F2, respectively.

Figure 5 shows the scheduling for the prices for 1st July 2015 [12]. The time interval of 30 minutes is chosen to coincide with the market prices. For all cases, the first noticeable observation is the IL procurement which only happens at time step 12. As expected, during noon, most of the consumption comes from PV. In the morning, during low space conditioning and low warm water demand, excess PV is sent back to the grid. Throughout the simulation, all temperatures and actuator constraints are satisfied. Furthermore, as an evidence of cost effective operation, one can observe that for the most amount of time the building/WWS schedules its consumption, so that it

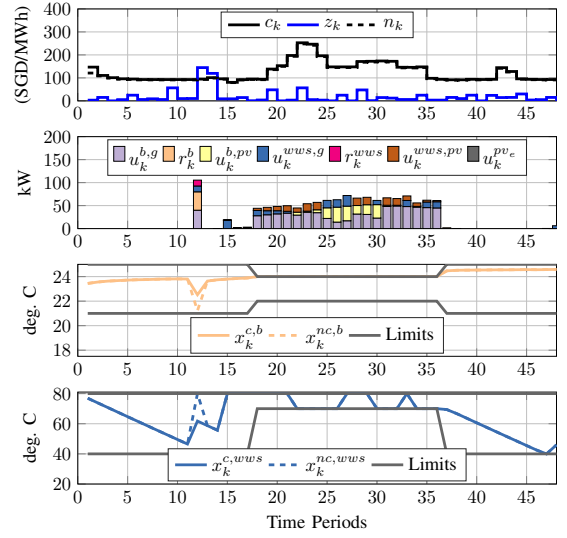


Fig. 5. Energy, Reserve and Nodal Prices from the EMC [12] (top-most). Control, reserve and PV power inputs into the building and WWS (2nd from top). Temperature evolution of thermal states of one zone of the building (2nd from bottom) and WWS, for both the curtailed and not-curtailed states (bottom-most).

stays at the allowable maximum/minimum temperature limits. The deviation from these cost-effective states is only observed for the instances of high monetary incentives or energy prices.

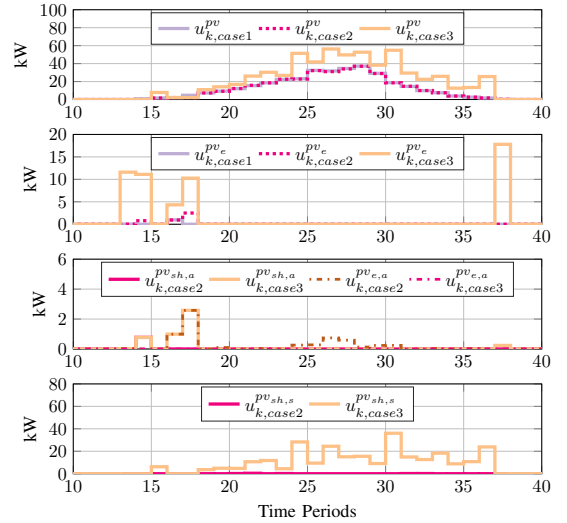


Fig. 6. Excess PV scheduling and its real time adjustment (see Section III)

Figure 6 shows the scheduling and mismatch of energy from the PV system for all three cases. Favorable for the distribution grid operation, case 3 does not inflict any extra PV feedback to the grid ($u_{case3,k}^{pv_{e,a}} = 0$). This positive effect on the grid is achieved at the cost of large real time adjusted energy flow ($u_{k,case3}^{pv_{sh,s}}$) from the grid (see Fig. 7). However, in contrast to case 3, case 2 demonstrates a closer behavior to the cost-optimal consumption strategy, i.e. case 1. Nevertheless, it can also be noticed that the PV feedback to the grid (reverse power

flow), due to the stochastic error in the forecast, becomes uncontrollable. The magnitude of the reverse power flow is higher at the beginning and closing of office hours, when the consumption requirements are lower. This information is particularly important for the distribution system and building operators, as it can help them optimize their individual systems accordingly.

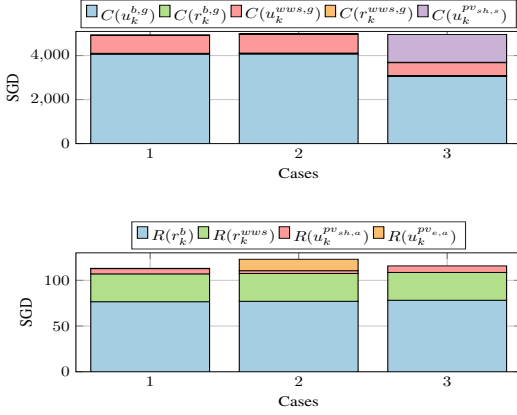


Fig. 7. The consumption cost (top) and revenue (bottom) for the whole month of July 2015.

To capture the long term effect on the cost of operation, Figure 7 shows the cost/revenue of the modeled system for all three cases. In comparison to case 1 (4,8382 SGD), the operational cost for case 2 (4,8799 SGD) and 3 (4,9383 SGD) shows an increase of 0.8% and 2%, respectively. Even though case 2 exhibits a better cost effectiveness than case 3, but it inflicts the POCC with 134.5 kW of unscheduled reverse power flow.

V. DISCUSSION

In this paper, we analyzed the influence of the imperfect PV forecast on the cost-optimal demand side services. Two forecast errors are introduced to study their implication on the control strategy. A moving horizon based stochastic error is found to introduce an extra reverse power flow back to the grid. Even though the introduction of the worst case error removes the reverse power flow, but it comes at the expense of higher cost of the overall operation. Hence, to account for the uncontrollability of renewables, it can be stated that the cost of optimality is to be compromised. Another conclusion can be made regarding the timing of energy requirements from loads, as synchronizing it with the nature of local PV improves the efficiency of the overall system.

The control strategy, simulation setup and analysis of this paper can still be considered as preliminary. As there are still few interesting questions, remaining to be answered, such as the influence of: (1) the distributed renewables and flexible loads in the overall distribution grid economics, (2) price uncertainty on the procurement strategies and (3) the activities of various actors with respect to the ownership of the distributed PV. We will pursue these research questions in the future.

VI. ACKNOWLEDGMENT

This work was financially supported by the Singapore National Research Foundation under its Campus for Research Excellence And Technological Enterprise (CREATE) programme. This work was also sponsored by National Research Foundation, Prime Ministers Office, Singapore under its Competitive Research Programme (CRP grant NRF2011NRF-CRP003-030, Power grid stability with an increasing share of intermittent renewables (such as solar PV) in Singapore).

REFERENCES

- [1] Luther, J. et. al., "Solar Photovoltaic (PV) Roadmap for Singapore (A Summary)," Solar Energy Research of Singapore (SERIS), Tech. Rep., 2013. [Online]. Available: https://www.nccs.gov.sg/sites/nccs/files/Roadmap_Solar_20140729.pdf
- [2] Liu, E. et. al., "Distribution System Voltage Performance Analysis for High-Penetration Photovoltaics Distribution System Voltage Performance Analysis for High-Penetration Photovoltaics," *Natl. Renew. Energy Lab.*, no. February, 2008.
- [3] M. Albadi and E. El-Saadany, "A summary of demand response in electricity markets," *Electr. Power Syst. Res.*, vol. 78, no. 11, pp. 1989–1996, 2008.
- [4] Torriti, J. et. al., "Demand response experience in Europe: Policies, programmes and implementation," *Energy*, vol. 35, no. 4, pp. 1575–1583, 2010.
- [5] Energy Market Authority, "Implementing Demand Response In The National Electricity Market of Singapore," EMA, Singapore, Tech. Rep., 2013. [Online]. Available: <http://tinyurl.com/zw5lmsn>
- [6] Castillo-Cagigal, M. et.al., "PV self-consumption optimization with storage and Active DSM for the residential sector," *Sol. Energy*, vol. 85, no. 9, pp. 2338–2348, 2011.
- [7] Vrettos, E. et. al., "Maximizing Local PV Utilization Using Small Scale Batteries and Flexible Thermal Loads," in *Eur. PV Sol. Energy Conf. Exhib.*, 2013. [Online]. Available: http://www.velasolaris.com/files/20013-10-pvsec_pres_13.pdf
- [8] Kaufmann, J. et. al., "Integrating Renewable Energy Requirements into Building Energy Codes," Tech. Rep. July, 2011.
- [9] Vrettos, E et. al., "Predictive Control of buildings for Demand Response with dynamic day-ahead and real-time prices," *Control Conf. (ECC), 2013 Eur.*, pp. 2527–2534, 2013.
- [10] Li, X. et. al., "PV integration in Low-Voltage feeders with Demand Response," in *2015 IEEE Eindhoven PowerTech*. IEEE, jun 2015, pp. 1–6. [Online]. Available: <http://ieeexplore.ieee.org/lpdocs/epic03/wrapper.htm?arnumber=7232251>
- [11] S. Swan, "Interruptible load: new partnerships for better energy management," *2005 Int. Power Eng. Conf.*, pp. 888–892 Vol. 2, 2005.
- [12] "Energy Market Company Singapore." [Online]. Available: <https://www.emcsg.com/>
- [13] Energy Market Authority, "Introduction to the National Electricity Market," Energy Market Authority, Singapore, Tech. Rep. October, 2010. [Online]. Available: https://www.ema.gov.sg/cmsmedia/Handbook/NEMS_111010.pdf
- [14] Singapore-Power, "Contestable Consumers: Market Settlement for PV Systems." [Online]. Available: <http://tinyurl.com/zfh94ht>
- [15] Hanif, S. et. al., "Model predictive control scheme for investigating demand side flexibility in Singapore," in *2015 50th Int. Univ. Power Eng. Conf.*, 2015, pp. 1–6.
- [16] Maasoumy, M. et. al., "Model-Based Hierarchical Optimal Control Design for HVAC Systems," *ASME 2011 Dyn. Syst. Control Conf. Vol. 1*, pp. 271–278, 2011.
- [17] Sturzenegger, David et. al., "Building Resistance-Capacitance Modeling (BRCM) ToolBox," 2012. [Online]. Available: <http://www.brcm.ethz.ch>
- [18] "Solar Energy Research Institute of Singapore (SERIS)." [Online]. Available: <http://www.seris.sg/>
- [19] Viessmann, "Viessmann Vitocell 300-V," Viessman, Tech. Rep., 2015. [Online]. Available: <http://tinyurl.com/gtuz2lh>
- [20] Lenzi, V. et. al., "Impacts of forecast accuracy on grid integration of renewable energy sources," *PowerTech (POWERTECH), 2013 IEEE Grenoble*, pp. 1–6, 2013.